



Published in final edited form as:

*PET Clin.* 2012 January ; 7(1): 119–126. doi:10.1016/j.cpet.2011.12.007.

## Prediction and Early Detection of Response by NMR Spectroscopy and Imaging

Seung-Cheol Lee, PhD<sup>a</sup>, Fernando Arias-Mendoza, MD, PhD<sup>b</sup>, Harish Poptani, PhD<sup>a</sup>, E. James Delikatny, PhD<sup>a</sup>, Mariusz Wasik, MD<sup>c</sup>, Michal Marzec, MD, PhD<sup>d</sup>, Stephen J. Schuster, MD<sup>e,f</sup>, Sunita D. Nasta, MD<sup>g</sup>, Jakub Svoboda, MD<sup>h,i</sup>, Owen A. O'Connor, MD, PhD<sup>j</sup>, Mitchell R. Smith, MD, PhD<sup>k</sup>, and Jerry D. Glickson, PhD<sup>a,\*</sup>

<sup>a</sup>Laboratory of Molecular Imaging, Department of Radiology, The University of Pennsylvania School of Medicine, B6 Blockley Hall, 423, Guardian Drive, Philadelphia, PA 19104-6069, USA

<sup>b</sup>Department of Radiology and Hatch Imaging Center, Columbia University College of Physicians & Surgeons, 710 West 168th Street, New York, NY 10032, USA

<sup>c</sup>Department of Pathology & Laboratory Medicine, The University of Pennsylvania School of Medicine, Philadelphia, 6 Founders, 3400 Spruce Street, Philadelphia, PA 19104, USA

<sup>d</sup>The Children's Hospital of Philadelphia, Abramson Research Building, 3516 Civic Center Boulevard, Philadelphia, PA 19104, USA

<sup>e</sup>Division of Hematology-Oncology, Department of Medicine, Hospital of the University of Pennsylvania, Philadelphia, PA 19104, USA

<sup>f</sup>Abramson Cancer Center of the University of Pennsylvania, 3400 Civic Center Boulevard, Philadelphia, PA 19104, USA

<sup>g</sup>Hospital of the University of Pennsylvania, 3400 Civic Center Boulevard, Philadelphia, PA 19104, USA

<sup>h</sup>Hospital of the University of Pennsylvania, Philadelphia, PA 19104, USA

<sup>i</sup>Department of Medicine, University of Pennsylvania School of Medicine, 3400 Civic Center Boulevard, Philadelphia, PA 19104

<sup>j</sup>Department of Hematology/Oncology, Columbia University Medical Center, 1130 Street Nicholas Avenue, ICRC 2216, New York, NY 10032, USA

<sup>k</sup>Lymphoma Service, Fox Chase Cancer Center, 333 Cottman Avenue, Philadelphia, Pennsylvania, 19111-2497, USA

### Keywords

Phosphorus-31 magnetic resonances spectroscopy; Hydrogen-1 magnetic resonance spectroscopy; Lactate; Choline

---

The authors' laboratory was the first to demonstrate that <sup>31</sup>P NMR spectroscopy was able to detect early metabolic changes in subcutaneous tumors in mice in response to chemotherapy, radiation therapy, and hyperthermia.<sup>1</sup> In addition, the authors and others<sup>2,3</sup> showed that nuclear magnetic resonance (NMR) detectable changes during untreated growth reflected

changes in tumor perfusion, energetics, and pH, which could serve as sensitive predictors of therapeutic response. These seminal observations were subsequently translated into the clinic and led to the initiation of a National Institutes of Health supported multi-institutional program to evaluate the potential utility of  $^{31}\text{P}$  magnetic resonance spectroscopy (MRS) for the prediction and early detection of therapeutic response. This program was initially headed by Dr Truman Brown at the Fox Chase Cancer Center and included Memorial Sloan-Kettering, Wayne State University, Duke, University of California in San Francisco (UCSF), Johns Hopkins, and The Royal Marsden and St George's Hospitals in London. Initially the study included 4 malignancies rGr exhibited approximately a 50:50 response rate—non-Hodgkin lymphoma (NHL), squamous cell carcinoma of the head and neck (HNSCC), soft tissue sarcomas (STS), and locally advanced breast cancer (LABC). Because of limited accrual, HNSCC, STS, and LABC were dropped from the study, and Wayne State, Duke, and UCSF left the study. However, the Radboud University Nijmegen Medical Center in the Netherlands joined the study. The participants call themselves Cooperative Group for NMR Spectroscopy of Cancer. While the participants in this program have continued to work together for over a decade, some have changed institutions. Dr Brown moved from Fox Chase to Columbia Presbyterian Medical Center and more recently to the Medical College of South Carolina, but a new principal investigator (PI), Dr Fernando Arias-Mendoza, has remained at Columbia. The Johns Hopkins Group under Dr Glickson moved to the University of Pennsylvania in 1996, and St George's group under Dr Griffiths recently transferred to Cambridge University in the United Kingdom. Despite changes of institutions among some of the participants, and the use of different commercial imaging systems (General Electric, Siemens, and Philips), a uniform protocol has been developed for acquisition and analysis of MRS data,<sup>4</sup> with statistical evaluation being performed at the PI institution (Columbia). Both the Columbia and University of Pennsylvania programs are participating in this report. Until now, all the  $^{31}\text{P}$  studies were performed on 1.5 T instruments, although future plans are to continue the studies at 3 T. Because of the limited sensitivity of  $^{31}\text{P}$  MRS, studies have been limited to large ( $3 \times 3 \times 3 \text{ cm}^3$ ) mostly superficial lesions in the axial, inginal, or head and neck lymph nodes. Data were generally analyzed from a single voxel, although data acquisition was performed by 2-dimensional chemical shift imaging followed by voxel shifting to optimally localize the tumor in one voxel (Fig. 1). Visualization of the tumor was achieved by  $T_2$ -weighted  $^1\text{H}$  magnetic resonance imaging (MRI). Recently, a number of institutions have initiated  $^1\text{H}$  MRS (lactate [Lac] or (total choline [tCho]) and MRI (diffusion-weighted imaging [DWI]), which can accommodate substantially smaller lesions (approximately  $1 \text{ cm}^3$  for Lac and tCho and smaller for DWI).

The scope and operational procedure has evolved over about 15 years of the study. Overall, more than 200 NHL patients have participated in the  $^{31}\text{P}$  MRS study. The initial plan was to perform MRS measurements before and after treatment, but it soon became apparent that because the examination required that the patient be confined in the magnet for about an hour, few patients returned for the follow-up examination. Therefore, the study focused on evaluating the utility of pre-treatment metabolic data for predicting complete response (CR) defined according to WHO criteria as complete disappearance of all detectable lesions and on time to treatment failure (TTF). Fig. 1 shows the  $^{31}\text{P}$  NMR spectrum of a typical NHL tumor in a human patient.

Based on animal data and anecdotal clinical reports, the ratio of phosphocholine (PCh) plus phosphoethanolamine (PEth), 2 phospholipid precursors, to total nucleoside triphosphate (NTP) (ie,  $[\text{PCh} + \text{PEth}]/\text{NTP}$  also called the phosphatemonoester/NTP or PME/NTP ratio) was chosen as the biomarker for predicting therapeutic response. Initially patients with all forms of NHL treated with any therapeutic modality or combination of modalities were accepted into the study. Remarkably, despite this diversity of tumor histology and treatment

method, the pretreatment PME/NTP ratio proved to be a robust predictor of response failure. When patients were stratified with respect to risk of tumor progression in accordance with the International Prognostic Index as low- (L), low-to-Intermediate (LI), high-to-intermediate (IH) and high- (H) risk and the PME/NTP values were plotted for each risk category, it was noted that simply drawing a line between the median of the L and IL PME/NTP ratios and extending this line to the HI and H risk categories segregated the PME/NTP ratios into 2 groups (Fig. 2).<sup>5</sup> With few exceptions, all the ratios above this line originated from tumors that were not destined to exhibit a CR, whereas those tumors whose PME/NTP ratios fell below this line were approximately equally distributed between patients with CRs and non-CRs (NCR). Thus with a sensitivity of 0.92 and specificity of 0.79, it was possible to predict CR or non-CR in these patients. An even better prediction has recently been achieved by defining an optimum cut-off value of PME/NTP for each tumor grade (Cooperative Group in NMR Spectroscopy of Cancer, unpublished data, 2011). However, in a more recent study of 27 patients with the most common form of NHL, diffuse large B-cell lymphoma all of whom were treated with RCHOP or “RCHOP-like” therapy, a similar analysis was able to predict CR or non-CR with a sensitivity of 1.0 and specificity of 0.90.

The key limitation of the <sup>31</sup>P MRS technique is its low sensitivity. To overcome this limitation, the University of Pennsylvania component of the Cooperative Group undertook preclinical <sup>1</sup>H MRS and MRI as well as <sup>31</sup>P MRS studies of human diffuse large B-cell lymphoma (DLBCL) xenografts in nude mice using the DLCL2 tumor model introduced by Mohammed and colleagues<sup>6,7</sup> Treatment of these xenografts with cyclophosphamide, hydroxydaunorubicin, oncovin (vincristine), prednisone or prednisolone (CHOP), rituximab (R), RCHOP, CHOP plus bryostatin (CHOPB) or radiation therapy (RTX) were evaluated using protocols similar to the clinical protocols except that the drug doses were slightly modified; the time per cycle of drug therapy was decreased from 3 weeks to 1 week because of the shorter doubling time of the tumor in the mouse, and the RTX was administered as a single 15 Gy bolus instead of multiple 2 Gy fractions.<sup>8-11</sup> Tumor volume, measured with calipers, was the response end-point. Relative response followed the order RTX>CHOPB>CHOP = RCHOP>R, with R producing only a slight growth delay. The <sup>1</sup>H MRS studies indicated that decreases in steady state lactic acid (Lac) were statistically significant following 1 cycle of therapy with CHOP, CHOPB, or within 24 hours following RTX, whereas treatment with R alone had no effect on Lac but decreased total choline (tCho), which was also decreased by RCHOP, CHOPB, or RTX. CHOPB and RTX also decreased the PME/NTP ratio of the tumor, but none of the other treatments had a significant effect on metabolites detected by <sup>31</sup>P MRS. Of potentially greatest clinical significance was the observation that with respect to treatment of the DLCL2 xenograft model with CHOP or RCHOP, which are the 2 most common therapies for DLBCL patients, Lac was selectively responsive to CHOP, whereas tCho was selectively responsive to R; hence, a decrease of Lac but an increase in tCho following RCHOP therapy could indicate rituximab resistance, which could be treated in the clinic with lenalidomide or other agents that restores immunologic response of NHL tumors. This principle is demonstrated in Fig. 3, which shows data from a DLBCL patient who was examined on a Monday, started RCHOP therapy on Wednesday and was re-examined on Friday. His tumor exhibited a 70% decrease in Lac and a 15% increase in tCho, suggesting that this patient may have been rituximab refractive, but no confirmatory data of this were obtained. The patient went on to exhibit a CR and is still in remission several months after treatment.

Recent <sup>13</sup>C MRS studies of the DLCL2 model using the 2-compartment analysis technique of Artemov and colleagues<sup>12</sup> demonstrate that the decrease in steady-state lactate levels following CHOP chemotherapy resulted from a 16% decrease in glycolytic flux and a 55% increase in lactate washout rate (S.C. Lee and J.D. Glickson, unpublished data, 2011);

hence, the changes in lactate levels appear to be perfusion driven and probably could be detected by dynamic contrast enhanced (DCE) MRI. Such studies are now in progress.

The University of Pennsylvania group has recently performed a pilot study of 1 chronic lymphocytic leukemia/small lymphocytic lymphoma (CLL/SLL) patient who had developed resistance to R. This patient was examined by  $^1\text{H}$  MRS/MRI at 5 time points in the UPCC-02408 protocol for restoring R-sensitivity with lenalidomide (Fig. 4A). Fig. 4B summarizes the NMR results. After 4 weeks of R following lenalidomide, tCho was decreasing throughout the R treatment portion of the protocol, and the tumor began to shrink after 4 cycles of R. These results are consistent with the authors' animal studies, but obviously data on more patients are required to draw definitive conclusions. The decrease in tumor volume is small, comes only late in the treatment schedule, and is preceded by decreases in tCho. The authors have also performed DWI measurements of the apparent diffusion constant (ADC) of this patient's tumor. The gradual increase in ADC after treatment with lenalidomide is consistent with restoration of R response (see Fig. 4B). In these preliminary studies, the authors only recorded the average ADC of the entire tumor; a detailed image multivoxel analysis of ADC values of coregistered data over the entire course of therapy is planned for the future.

It is important to note that the authors are dealing with an indolent lymphoma for which complete regression may not be anticipated. The key point is that the disease is not progressing. The authors are intrigued by the increase in tCho during the initial lenalidomide treatment. Lenalidomide may produce an inflammatory response that caused this increase. Increases in Lac might have confirmed this, but unfortunately technical problems interfered with obtaining these data. The authors plan to pursue this in future experiments.

The utility of 2 forms of MRI (DWI and  $T_2$ -weighted [T2WI]) was evaluated on DLCL2 xenografts treated with CHOPB.<sup>13</sup> These imaging methods produce tumor images showing submillimeter in-plane resolution at acquisition times on the order of 10 minutes. Bryostatins produce a more robust response of this tumor model to CHOP chemotherapy by inhibiting multidrug resistance or Bcl-2 expression.<sup>7</sup> A significant increase in the ADC was detected by DWI following only 1 cycle of CHOPB, whereas T2WI required 2 therapy cycles to detect a statistically significant but anomalous decrease in the average  $T_2$ .<sup>13</sup> However, the most interesting observation was that in 3 of the 5 tumors examined, the changes in ADC or  $T_2$  were not uniform over the entire tumor but were limited to distinct regions of the tumor. This regional response pattern could be due to various causes including heterogeneity in tumor perfusion, oxygenation, or apoptotic ability or drug resistance (which are energy- and hence perfusion-dependent). The exact mechanism producing this heterogeneity is under examination, but it is apparent that if, for example, it proves to be related to perfusion, then there are various interventions that could be used to produce a more homogeneous and, therefore, extensive response of the tumor. Thus, image-guided therapy is a distinct possibility if not a probability for the future.

About 30% of all the new cancer drugs under development by pharmaceutical companies target signal transduction pathways. These drugs usually act by inhibiting key kinases that modify critical cell properties such as proliferation, apoptosis, angiogenesis, bioenergetics, gene expression, protein expression, and others. However, there are no noninvasive imaging methods for monitoring the actual kinase inhibition in the malignant cells in patients. There is, however, a great need to monitor these processes within the individual patient. To develop such a method, the authors proceeded on the assumption that to modify vital cellular functions, signal transduction pathways had to modify cellular metabolism; cellular metabolism can be monitored by NMR and positron emission tomography (PET) methods. The goal was, therefore, to identify specific metabolic pathways that were modified when

specific signaling pathways were inhibited. As proof of principle, the authors chose the mTORC1 pathway, which is selectively inhibited by rapamycin and its analogs. Treatment with 7 doses of rapamycin (10 mg/kg  $\times$  2 doses/d) of mice transplanted with the human DLCL2 lymphoma cell line produced a 90% decrease in tumor Lac detected by  $^1\text{H}$  MRS (Lee S-C, Marzec M, Liu X, et al. submitted for publication). There was no significant change in tCho. Gene chip and Western blot analysis indicated an approximate 35% decrease in the expression of hexokinase-2, the key enzyme involved in regulating tumor glycolysis. A number of other glycolytic enzymes exhibited smaller decreases in expression following rapamycin treatment including phosphofructokinase (15% to 20%), enolase 1 (18%) and pyruvate kinase (5%). There was a small decrease in choline kinase and a small increase in phospholipase A<sub>2</sub>. Therefore, the glycolytic pathway appears to be selectively inhibited. Similar findings were made with another human lymphoma cell line Ramos. Thus, it appears that inhibition of mTOR can be monitored selectively by  $^1\text{H}$  MRS using lactate imaging methods<sup>14-16</sup> and probably also by fluorodeoxyglucose (18F) or 2-deoxy-2-(18F)fluoro-D-glucose (FDG) PET.

In summary, the authors have shown that pretreatment  $^{31}\text{P}$  MRS can predict about two-thirds of the response failures among human NHL patients. These patients could be directed to more vigorous therapeutic regimens followed by bone marrow transplantation or to experimental new therapeutic agents. Phosphorus-31 NMR is limited to large superficial tumors and only provides a predictor of response failure rather than successful response unless the method is applied to populations of patients with DLBCL tumors treated with RCHOP or equivalent therapy. Proton NMR data can be used to monitor much smaller tumors in any site in the human body. Proton spectroscopy has 2 response markers, lactate and choline, which can selectively detect response to CHOP chemotherapy and rituximab immunotherapy, respectively. This may provide a noninvasive method for detecting patients refractory to rituximab therapy who can be treated with thalidomide-related agents that restore rituximab response. Finally, the authors have demonstrated a general strategy for noninvasively monitoring response to inhibitors of specific signal transduction pathways by monitoring the corresponding metabolic pathway that is modified by signal transduction inhibition. The authors have demonstrated that in the case of mTOR, inhibition of this signaling pathway can be detected by inhibition of glycolysis, which can be detected by  $^1\text{H}$  MRS lactate imaging or FDG PET.

## Acknowledgments

This work has been supported by NIH grants CA101700, CA41078CA041078 and CA118559, CA89194, CA96856. Animal studies were performed at the Small Animal Imaging Facility of the University of Pennsylvania that is operated with partial support from an NCI Small Animal Resource grant. Much of this research has been conducted by members of the Cooperative Group on 5U24CA08315-0708 and as a core facility of the Abramson Comprehensive Cancer Center that is supported by 5P30CA016520-34. Clinical studies have been performed by the NMR Spectroscopy in Cancer Cooperative Group that includes the following participants: Columbia University (Fernando Arias-Mendoza), Memorial Sloan-Kettering Cancer Center (Jason A. Koutcher, Kirsten Zakian, Amita Shukla-Dave), The Royal Marsden Hospital, London, UK (Martin O. Leach, Geoffrey S. Payne, Adam J. Schwarz, David Cunningham), CR UK Cambridge Research Institute, Cambridge, United Kingdom (John R. Griffiths, Marion Stubbs), Radboud University Nijmegen Medical Center, The Netherlands (Arend Heerschap), Medical University of Charleston, SC (Truman R. Brown), The University of Pennsylvania (Harish Poptani, Seung-Cheol Lee and Jerry D. Glickson).

## References

1. Ng TC, Evanochko WT, Hiramoto RN, et al. P-31 NMR-spectroscopy of in vivo tumors. *J Magn Reson.* 1982; 49(2):271–86.
2. Evelhoch JL, Sapareto SA, Nussbaum GH, et al. Correlation between  $^{31}\text{P}$  NMR spectroscopy and  $^{15}\text{O}$  perfusion measurements in the RIF1 murine tumor in-vivo. *Radiat Res.* 1986; 106(1):122–31. [PubMed: 3961103]

3. Glickson, JD.; Wehrle, JP.; Rajan, SS., et al. NMR spectroscopy of tumors. In: Pettegrew, JW., editor. NMR in Biomedical Research. New York: Springer-Verlag; 1989. p. 253-307.
4. Arias-Mendoza F, Zakian K, Schwartz A, et al. Methodological standardization for a multi-institutional in vivo trial of localized P-31 MR spectroscopy in human cancer research. In vitro and normal volunteer studies. NMR Biomed. 2004; 17(6):382–91. [PubMed: 15386624]
5. Arias-Mendoza F, Smith MR, Brown TR. Predicting treatment response in non-Hodgkin's lymphoma from the pretreatment tumor content of phosphoethanolamine plus phosphocholine. Acad Radiol. 2004; 11(4):368–76. [PubMed: 15109009]
6. Al-Katib AM, Smith MR, Kamanda WS, et al. Bryostatin 1 down-regulates mdr1 and potentiates vincristine cytotoxicity in diffuse large cell lymphoma xenografts. Clin Cancer Res. 1998; 4(5): 1305–14. [PubMed: 9607591]
7. Mohammad RM, Wall NR, Dutcher JA, et al. The addition of bryostatin 1 to cyclophosphamide, doxorubicin, vincristine, and prednisone (CHOP) chemotherapy improves response in a CHOP-resistant human diffuse large cell lymphoma xenograft model. Clin Cancer Res. 2000; 6(12):4950–6. [PubMed: 11156256]
8. Huang MQ, Nelson DS, Pickup S, et al. In vivo monitoring response to chemotherapy of human diffuse large B-Cell lymphoma xenografts in SCID mice by H-1 and P-31 MRS. Acad Radiol. 2007; 14(12):1531–9. [PubMed: 18035282]
9. Lee SC, Huang MQ, Nelson DS, et al. In vivo MRS markers of response to CHOP chemotherapy in the WSU-DLCL2 human diffuse large B-cell lymphoma xenograft. NMR Biomed. 2008; 21(7): 723–33. [PubMed: 18384181]
10. Lee SC, Delikatny EJ, Poptani H, et al. In vivo H-1 MRS of WSU-DLCL2 human non-Hodgkin's lymphoma xenografts: response to rituximab and rituximab plus CHOP. NMR Biomed. 2009; 22(3):259–65. [PubMed: 19040203]
11. Lee SC, Poptani H, Jenkins WT, et al. Early detection of radiation therapy response in non-Hodgkin's lymphoma xenografts by in vivo 1H magnetic resonance spectroscopy and imaging. NMR Biomed. 2010; 23(6):624–32. [PubMed: 20661875]
12. Artemov D, Bhujwalla ZM, Pilatus U, et al. Two-compartment model for determination of glycolytic rates of solid tumors by in vivo C-13 NMR spectroscopy. NMR Biomed. 1998; 11(8): 395–404. [PubMed: 10221582]
13. Huang MQ, Pickup S, Nelson DS, et al. Monitoring response to chemotherapy of non-Hodgkin's lymphoma xenografts by T-2-weighted and diffusion-weighted MRI. NMR Biomed. 2008; 21(10): 1021–9. [PubMed: 18988250]
14. Serrai H, Nadal-Desbarats L, Poptani H, et al. Lactate editing and lipid suppression by continuous wavelet transform analysis: application to simulated and H-1 MRS brain tumor time-domain data. Magn Reson Med. 2000; 43(5):649–56. [PubMed: 10800029]
15. Pickup S, Lee SC, Mancuso A, et al. Lactate imaging with Hadamard-encoded slice-selective multiple quantum coherence chemical-shift imaging. Magn Reson Med. 2008; 60(2):299–305. [PubMed: 18666110]
16. Mellon EA, Lee SC, Pickup S, et al. Detection of lactate with a hadamard slice selected, selective multiple quantum coherence, chemical shift imaging sequence (HDMD-SELMQC-CSI) on a clinical MRI scanner: application to tumors and muscle ischemia. Magn Reson Med. 2009; 62(6): 1404–13. [PubMed: 19785016]

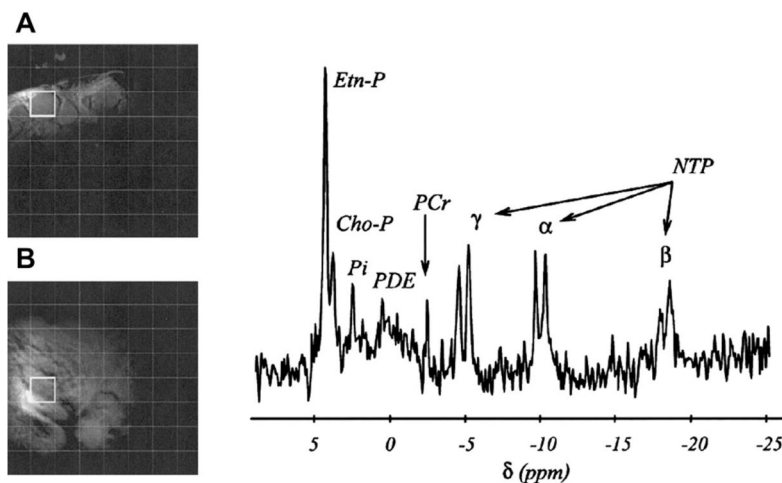


**Fig. 1.** Example of an in vivo localized  $^{31}\text{P}$  magnetic resonance spectroscopy study of a non-Hodgkin lymphoma. Insets (A) and (B) show two orthogonal magnetic resonance images (axial and coronal, respectively), illustrating tumor localization, in this case the right inguinal area. The images were overlaid with the  $^{31}\text{P}$  3-dimensional localization chemical shift imaging (CSI) grid, a cubic matrix with 8 steps per spatial dimension with a nominal cubic voxel of  $30\text{ mm}^3$ . The  $^{31}\text{P}$  spectrum was sampled from the single tumor voxel projected on the images shown by a thick-lined square. The assignments are phosphoethanolamine (**Etn-P**) and phosphocholine (**Cho-P**) in the phosphomonoester region; inorganic phosphate (**Pi**); phosphodiester region (**PDE**); phosphocreatine (**PCr**); and phosphates  $\alpha$ ,  $\beta$ , and  $\gamma$  of nucleotide triphosphates (**NTP**). The chemical shift ( $\delta$ ) is expressed in parts per million (**ppm**) using the phosphoric acid as reference at 0 ppm (internal reference  $\text{P}\alpha$  of NTP at  $-10.01\text{ ppm}$ ). The leftover glitch of PCr in the spectrum is minimal contamination from neighboring voxels caused by the CSI point spread function. The (Etn-P Cho-P)/NTP ratios reported throughout the article were obtained by summing the integrals of the Etn-P and Cho-P signals in the tumor spectra and dividing the result by the integral of the  $\beta$ -phosphate of NTP (assignments in bold). (From Arias-Mendoza F, Smith MR, Brown TR. Predicting treatment response in non-Hodgkin's lymphoma from the pretreatment tumor content of phosphoethanolamine plus phosphocholine. *Acad Radiol* 2004;11(4):370; with permission.)

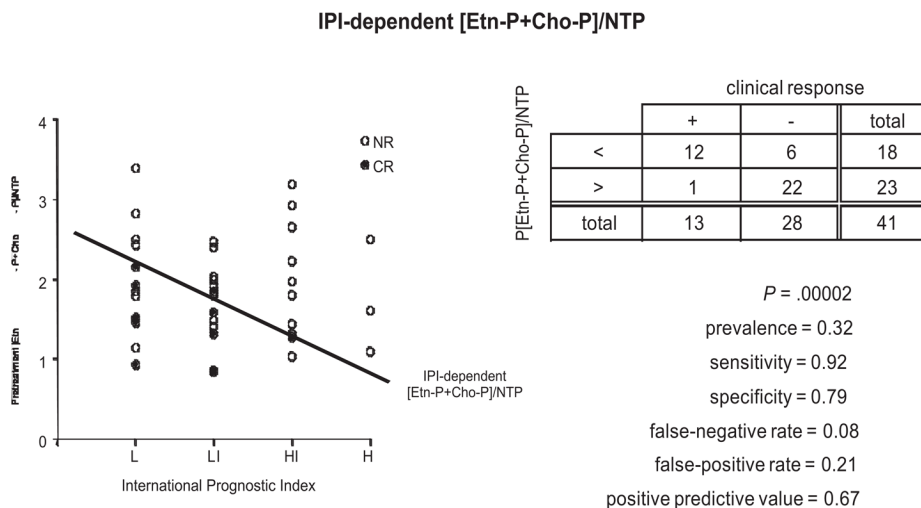


**Fig. 2.** Correlation of the international prognostic index (IPI) and the pretreatment phosphatemoester/nucleoside triphosphate per patient in the whole non-Hodgkin lymphoma cohort. The long-term response to treatment outcome of each patient was also plotted as CR, complete response (*filled circles*) and noncomplete responders (*open circles*). Tumors were stratified on the basis of the IPI as low grade (L), low-to-intermediate (LI), high-to-intermediate (HI) and high-grade (H) tumors. A line was drawn between the medians of the L and LI points and extended through the HI and H columns. This line was a useful threshold for predicting failure to exhibit a CR.



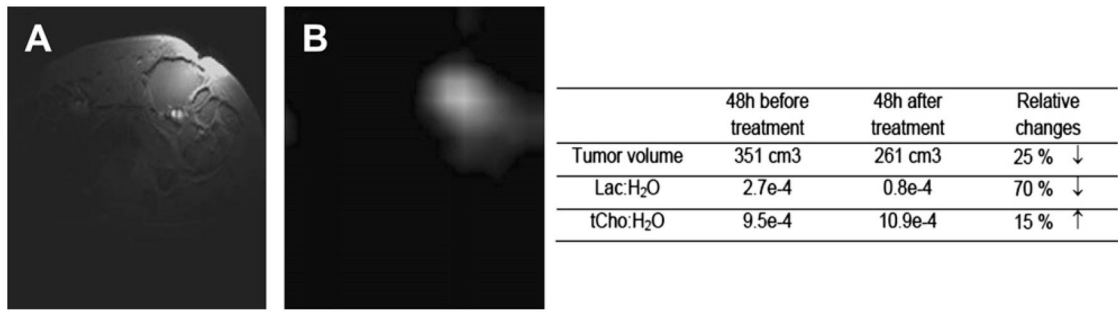


**Fig. 3.** 63-year-old man with inguinal node diffuse large B-cell lymphoma. (A) T2-weighted image, echo time = 15 milliseconds, repetition time = 3000 milliseconds (B) Lactate image measured with Had-SelMQC- chemical shift imaging sequence.

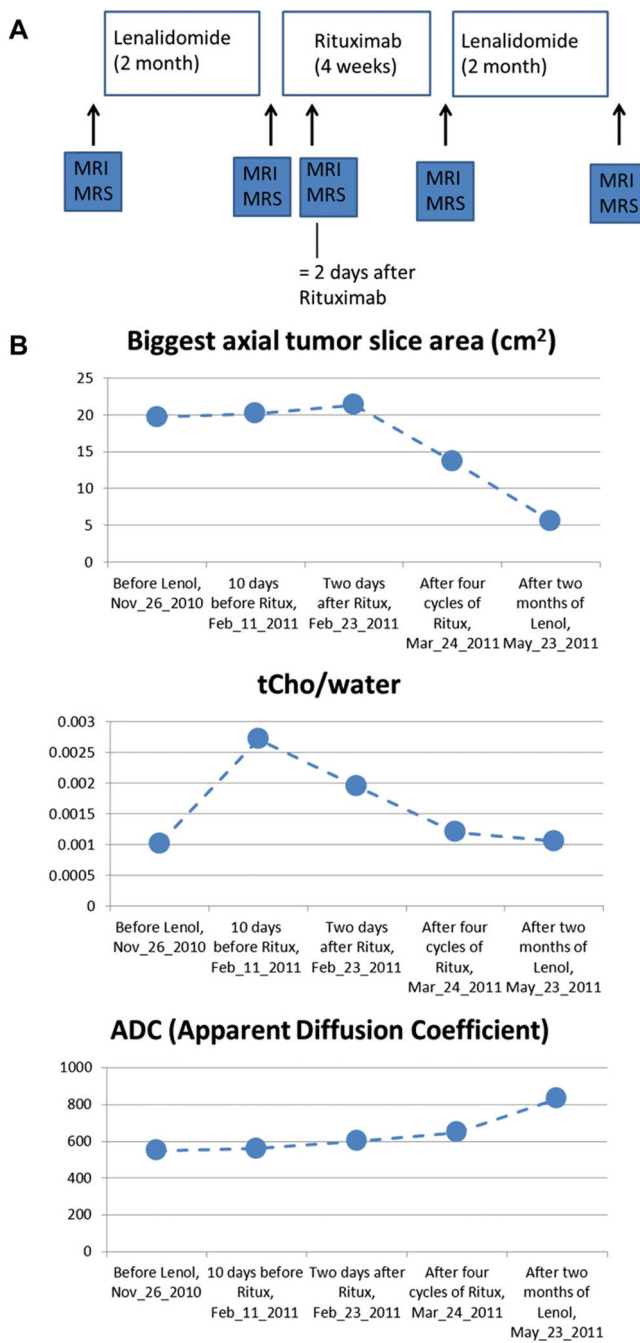


**Fig. 4.** (A) Treatment protocol and time points for magnetic resonance imaging/magnetic resonance spectroscopy studies of CLL/SLL patient. Results shown in Fig. 3B. (B) Summary of tumor size, total choline (tCho) and apparent diffusion constant (ADC) of a patient on 5 examinations.